View metadata, citation and similar papers at core.ac.uk

brought to you by CORE

provided by NASA Technical Reports Server

Final Report

on

LIQUID METAL EMBRITTLEMENT GRANT

NASA-Ames NGR 05-020-549

prepared by

Professor William A. Tiller
Department of Materials Science & Engineering
Stanford University
Stanford, California 94305

SU-DMS-74-R-22

November 1, 1973

(NASA-CR-137429) LIQUID MEIAL EMBRITTLEMENT Final Technical Report (Stanford Univ.) 30 p HC $4.50 CSCL 11F

N74-21116

Unclas
G3/17 16495

Final Report

Liquid Metal Embrittlement

Grant NASA-Ames NGR 05-020-549

Introduction

The objective of this research was to develop a theoretical understanding of why certain liquid metals embrittle certain solid metals and to generate a procedure for predicting rates of crack propagation in such systems. The studies were to include both theoretical and experimental portions. However, the graduate student, Mr. Donald Nason, worked on the project for only 5 months and then left the country to pursue a special job opportunity. No substantial progress had been made before he left and it wasn't possible to have someone else step in and pick up where Nason left off without excessive time delays. Thus, at that point in time, the principal investigator decided to pursue a completely theoretical program for the duration of the contract. This necessitated some reevaluation of the order in which work should be done and involved attention being placed on the fundamentals of stress corrosion cracking. The path decided upon is outlined in the next section.

Overview

Generally, we know that, as a crack propagates, it alters the strain energy storage in the surrounding matrix, it generates defects and releases defects stored in the surrounding matrix and it creates new surface. Of course, the crack will only propagate if the free energy of the system is lowered by the propagation of such a "negative dendrite." In the evaluation

of the excess energy stored in the metal volume, one must consider the traction forces acting across the interior domain of the crack faces. Although this adhesive force is trivial for non-metals, it may be substantial for metals and needs evaluation. This force is also influenced by the type of fluid media included in the crack space because of screening effects. For example, if the fluid is a liquid metal, the screening is much more effective than for a simple electrolyte and these adhesive forces may be diminished by a large factor (needs evaluation).

The inhomogeneous stress field at the tip of a crack is expected to produce an electrostatic potential in the matrix and along the crack surface because of electron redistribution. This will give rise to local electron circulating currents when the inner crack space is filled with a liquid metal. By the type of vacancy-failure mechanism that one sees in microelectronic systems, voids may be formed ahead of the advancing crack tip and accelerate the failure process. This situation definitely needs evaluation to determine the magnitudes of the circulating currents which are operative. Finally, the actual atomic process of crack surface translation; i.e., surface diffusion, volume vacancy diffusion, dissolution or the unzipping of bonds, needs evaluation for the liquid metal case.

Because of the foregoing, it was decided that several difficult problems merited serious attention and these were pursued during the period of the contract. They are:

1. Investigate the change in the electrochemical potential of an electron in a metal due to a change in stress level and identify the procedure for determining the resultant electrostatic potential variation along the crack surface.

This latter involves coupling relationships between the stress field and the electrostatic field.

2. Investigate the change in local chemistry and interfacial energy due to atomic redistribution in the liquid and evaluate the altered state of surface roughening via this atomic redistribution, stress and electron density changes.

3. Evaluate the circulating current intensity and its consequences arising from the electrostatic potential variation along the wall of the crack

Theoretical Studies

1a. Coupled Elastic-Electrostatic Equations

Following the approach of Dessler et al.[1] who considered gravitationally-induced electric fields in conductors, one can readily modify the basic elastic equilibrium equations to include excess charge effects. Dessler et al.[1] wrote the energy of a macroscopic sample, U, in terms of the number of electrons, n, needed for neutrality, strain, ϵ, and number of excess electrons, ν^*, as

$$U = \int u(n,\epsilon,\nu^*)\, d\tilde{x} + \tfrac{1}{2} e^2 \int \nu^*(\tilde{x})\nu^*(\tilde{y}) \mid \tilde{x}-\tilde{y} \mid^{-1} d\tilde{x}d\tilde{y} - e \int \nu^*(x)\, \phi'(\tilde{x})\, d\tilde{x} \qquad (1)$$

where $\tilde{x}$ represents the generalized coordinate. Here, the second term represents the uncompensated charge in different incremental volume elements, j and k say (R_{jk}^{-1} is the mean inverse distance between these two volume elements). ϕ' represents the average electrostatic potential in the j^{th} element due to any "external" charges (ϕ' also includes the average electrostatic potential in the j^{th} elemenc arising from the nonspherical charge distribution in the crystal unit cells). Finally, u_j, is the energy of the j^{th} element minus the

contribution to the interaction energy of its excess charge enumerated above. Equation 1 is the fundamental relationship which leads to equations determining the ground state of the material when the energy is minimized. In the ground state, U is invariant to the first order variations in the parameters subject to any imposed constraints.

When the energy density in eq. 1 is expanded up to quadratic terms in the stresses and ν^*, the result is

$$u = u_0 + \tfrac{1}{2}\sigma_{ij}\epsilon_{ij} + \mu\nu^* + \tfrac{1}{2}\mu_{\nu^*}\nu^{*2} - \mu_n n_0 \epsilon_{ij}\nu^* \quad (2)$$

where μ is the chemical potential of the electrons, $\mu_{\nu^*} = \partial\mu/\partial\nu^*$, and $\mu_n = \partial\mu/\partial n$ (with the derivatives evaluated at $\nu^* = 0$, $n = n_0$), σ_{ij} is the stress tensor and ϵ_{ij} is the strain tensor. When eq. 2 is inserted in eq. 1 and the variations of U with respect to ν^* and ϵ_i are set equal to zero, we obtain

$$\mu + \mu_{\nu^*}\nu^* - n_0\mu_n\epsilon_{ii} - e\phi = \text{const.} \quad (3)$$

The variational equation for ϵ_i yields

$$\partial_j \sigma_{ij} - n_0\mu_n \partial_i \nu^* = 0 \quad (4a)$$

which can be put in the more convenient form

$$(K + \frac{4}{3}E^*)\,\nabla\nabla\cdot\epsilon - E^*\,\nabla\times(\nabla\times\epsilon) - n_0\mu_n\nabla\nu^* = 0 \quad (4b)$$

where K and E^* are the moduli of hydrostatic compression and rigidity respectively. We gain a third governing equation utilizing the connection between charge density and macropotential via Poisson's equation

$$\nabla^2\phi_{\nu^*} = \frac{4\pi e\nu^*}{\epsilon^*} \quad (5)$$

where ϵ^* is the effective dielectric constant of the medium and ϕ_{ν^*} is that electrostatic potential associated with the excess charge distribution ν^*. The total potential ϕ is given by

$$\phi = \phi_{\nu^*} + \phi_D \tag{6}$$

where ϕ_D is due to fixed dipoles distributed on the surfaces or in the volume of the material. Equations 3, 4, 5 and 6 constitute a coupled set determining the ground state of the elastic (isotropic) solid. In these equations, $\mu_n \approx \frac{2}{5}\mu_{\nu^*}$ and

$$\mu_{\nu^*} = \frac{\partial}{\partial \nu^*}\left[\frac{h^2}{2m}\left(\frac{3(u+\nu^*)}{8\pi}\right)^{2/3}\right]_{\nu^*=0}$$

This coupled set of equations indicate that, given an inhomogeneous stress distribution, a natural electrostatic field will be generated which will, in turn, alter the stress distribution. Thus, even in a metal, a crack tip under stress will develop a voltage variation along the surface of the crack. This does not cause electron motion inside the metal because this voltage is, in fact, needed to bring about a constant electrochemical potential for the electrons. However, it does influence ion motion on the surface of the crack and ion plus electron motion in the media within the crack gap. We can see in this the explanation for crevice corrosion. A curved notch contains surface dipoles which produce ϕ_D in the metal; electron screening leads to a ν^* distribution which leads to a naturally developed stress and strain, σ and ϵ. This stress distribution and electrostatic potential distribution on the surface of the metallic notch is the driving force for electrochemical action in the notch fluid and thus continuous corrosion.

It is possible to uncouple this set of 4 equations so that they can be

solved one at a time. However, this step is only just now being taken for certain practical geometries and loading situations.

1b. Stress Effects on Electron Energy States

The average energy per electron of a monovalent metal as a function of the dimensionless atom radius, r_s, (radius of sphere containing 1 electron) is

$$E(r_s) = E_o(r_s) + E_k(r_s) + E_e(r_s) + E_c(r_s) + E_{co}(r_s) \quad (7a)$$

$$\frac{r_s}{a_o} = \left[\frac{4}{3}\pi\frac{V}{N}\right]^{1/3} = A/N^{1/3} \quad (7b)$$

where N is the numbe· of free electrons in the volume V, a_o is the Bohr radius (a_o = 0.529A°), E_o is the lowest energy state (ground state) for an electron in the system, E_k, E_e and E_c are kinetic, exchange and correlation energies of the electron respectively and E_{co} is the term due to the overlap repulsion and van der Waals' attraction of the ionic cores plus a Coulomb term which is just the self-potential energy of the charge distribution within an atomic polyhedron. Using the Wigner[2] approximation, we have

$$E(r_s) - E_o(r_s) = \frac{2.21}{r_s^2}\alpha - \frac{0.916}{r_s} - \frac{0.88}{r_s+7.8} + E_{co}(r_s) \text{ Rydbergs} \quad (8)$$

where $\alpha = m/m^*$ and m^* is the effective mass of the electron at small electron wave number. Since the electrons are very nearly free for monovalent metals, one often sets $\alpha = 1$. Although one can generally neglect E_{co} (except for the Coulomb part = $+ 1.2/r_s$) for the alkali metals, it cannot be for the other monovalent metals, Cu, Ag and Au, even though the valence electron wave functions in these metals approximate almost as closely to free electron functions as they do in the alkali metals. This is because the ion cores, especially

the outermost d sub-shells in Cu, Ag and Au are so large that neighboring cores overlap appreciably. It is therefore not permissible to treat the interaction of the ion-cores as if they were point charges (procedure leading to eq. 8). Strictly speaking, the outermost d-electrons in these metals should be treated in the same way as the valence electrons but, since they are not free, such a calculation is not possible at this time.

For polyvalent metals, eq. 8 can be generalized for the valence Z. The kinetic, exchange and correlation energies are changed by substituting $Z^{-1/3}r_s$ for r_s; the Coulomb term is changed by substituting $Z^{-1}r_s$ for r_s and the E_o term is unchanged. We should expect eq. 8 to be an even worse approximation for a polyvalent metal because the electrons occupy states in more than one Brillouin zone and the energy variation with wave number is no longer a simple parabola.

From eq. 8, neglecting E_{co} except for the Coulomb part, it is possible to calculate various quantities (at absolute zero) and compare with the experimental results. The energy $E(r_s)$ passes through a minimum (see Fig. 1) at a radius r_o which corresponds to the equilibrium lattice constant. Using this procedure, calculated and experimental values of the cohesive energy, S^*, for the alkali metals are in good agreement. The cohesive energy is defined as the energy required to dissociate the metal, at absolute zero, into free atoms. The zero of energy in the computation corresponds to infinite separation of ion-cores and valence electrons. This requires the use of a quantity defined similarly for a free atom which is just the ionization energy (which is negative). The cohesive energy per electron, S^*, is thus given by

$$S^* = I - E(r_o) \qquad (9)$$

Our goal is to determine the direction of electron redistribution at the tip of a crack under loading conditions. It is also to determine the magnitude of the electrostatic potential change along the crack surface. To develop accurate magnitudes, we must utilize the results of the previous section (1a); however, that is beyond our present computational ability so we shall evaluate the effect using uncoupled physics and the thermodynamics of homogeneous systems.

To proceed, we need to evaluate the electrochemical potential of the electron, η_e, given by

$$\eta_e = \mu_e - e\phi_c \tag{10}$$

where e is the electronic charge, ϕ_c is the macropotential of the solid due to the electrical double layer at the external surface and μ_e is chemical potential of the electron (Fermi energy). In terms of eq. 7, we have

$$-e\phi_c(r_s) = E_0(r_s) \tag{11}$$

and

$$\mu_e = \left(\frac{\partial F_0}{\partial N}\right)_{V,T=0} = \frac{5}{3}E_k + \frac{4}{3}E_e + \left[1.33 - \frac{2.6}{r_s + 7.8}\right]E_c \quad \text{Ryd} \tag{12}$$

where

$$F_0 = N[E-e\phi]_o \tag{13}$$

is the Helmholtz free energy for the system. In eq. 12, E_{co} has been neglected. The proper energy diagram relating these quantities is given in Fig. 2. This is an energy diagram for the metal electron relative to the zero point energy of an electron at infinity outside the metal. We can also see the outer or contact potential (Volta potential), Φ_0, and the electron work function, Φ_w, which is the energy difference between just inside the surface to just outside

the surface.

Lang and Kohn[3] have recently evaluated the magnitude of ϕ_c for a number of simple metals first using a jellium model and then including effects of the ion cores (gives $\Delta\phi = \phi_c - \phi_0$) by using simple pseudopotential theory. For simples metals (Li, Na, K, Rb, Cs, Al, Pb, Zn, Mg), agreement of ϕ_w and the experimental data is good even though E_{co} in eq. 7 was completely neglected; however, for the noble metals, the computed ϕ_w are $\sim$ 25% too low. At the free surface of a metal, the electron redistribution, illustrated in Fig. 3a for the jellium model, produces the electrostatic potential across the interface illustrated in Fig. 3b.

From eqs. 10 and 11, we have

$$\frac{d\eta_e}{dr_s} = \frac{d\mu_e}{dr_s} + \frac{dE_0}{dr_s} \tag{14}$$

With the aid of Fig. 1, this can be evaluated at the equilibrium radius $r_s = r_0$ where $dE/dr_s = 0$ at $r_s = r_0$. Neglecting E_{co} for the moment, this leads to

$$\left(\frac{dE_0}{dr_s}\right)_{r_0} = -\left[\frac{d}{dr_s}(E_k + E_e + E_c)\right]_{r_0} \tag{15}$$

Thus, at $r_s = r_0$, we have

$$\left(\frac{d\eta_e}{dr_s}\right)_{r_0} = \left(\frac{d\mu_e}{dr_s}\right)_{r_0} - \left[\frac{d}{dr_s}(E_k + E_0 + E_c)\right]_{r_0}$$

$$= \frac{2}{3}\frac{dE_k}{dr_s} + \frac{1}{3}\frac{dE_e}{dr_s} + \frac{1}{3}\frac{dE_c}{dr_s} - \frac{d}{dr_s}\left[\frac{2.6\,E_c}{r_s - 7.8}\right] \text{ at } r_s = r_0 \tag{16a}$$

$$= -\frac{2.95}{r_0^2} + \frac{0.305}{r_0^2} + \frac{0.29}{(r_0 + 7.8)^2} - \frac{4.6}{(r_0 + 7.8)^3} \text{ Ryd} \tag{16b}$$

Equation 7 has been utilized here and, if we wish to include the Coulomb part of E_{co}, we must add $-1.2/r_o^2$ to the R.H.S. of eq. 16.

A plot of eq. 16b (for monovalent systems) is given in Fig. 4. We see that $(d\bar{\eta}_e/dr_s)_{r_o} < 0$ for the general range of r_o and that the magnitude is significantly affected by neglect of the Coulomb contribution. From this result, we can see that, within a strained metal, electrons will flow from regions of compression to regions of tension. Thus, if we consider two samples of constant N but different r_s in vacuum as represented in Fig. 5, connecting the two by a wire will lead to a flow of electrons from the sample with the smaller r_s to that with the larger. Likewise, if we consider electron transfer through the vacuum phase, the sample with the smaller r_s will have the larger ϕ_w which, from Fig. 2, means that it will have the smaller ϕ_o. Thus, the sample with the larger r_s will appear to have the more positive surface potential so that electrons will flow, via the vacuum, from the material with the smaller r_s to that with the larger. Thus, for a clean surface, before any electrons have been transferred, the tip of a crack would appear positively charged and the voltage would decrease as one moves away from the tip towards the root of the crack. However, the transfer of electrons to the interior metal adjacent the crack tip will create a potential of the opposite sign. The resultant sign of the voltage on the surface will depend upon the magnitude of these two effects and cannot be determined without detailed information concerning the stress distribution and the surface contour.

In the most general situation, the surface potential, ϕ_s, in the vicinity of the notch tip, will be given by

$$\phi_s = \phi'_{\nu*} + \phi'_c + \phi'_A + \phi'_d \qquad (17)$$

where the primes refer to the fact that we are dealing with a curved surface instead of a flat surface, ϕ_A refers to the dipole potential due to surface adsorption, ϕ_d refers to the dipole potential due to the passage of dislocations through the surface (plastic strain) and ϕ_{v^*} is that associated with electron redistribution. In eq. 17, the first term is always negative and the second always positive, the third may be either positive or negative and the fourth is generally found to be negative.

To conclude this section, we have developed a rigorous and reliable mode of description for the electrostatic potential along the crack surface. However, a specific situation and the solution to section (1a) is needed before a good quantitative measure can be forthcoming. Approximate computations indicate that a flat surface would change by ~ 10-50 mv per % volume tensile strain[4].

2. Crack Propagation Via Surface Roughening

The classical picture of crack propagation is that of atoms gradually separating from each other along some dividing plane as illustrated in Fig. 6. Long before this happens, a different mechanism is likely to come into play. This is the familiar surface roughening mechanism whereby atoms in a smooth surface jump out of the surface to produce a surface vacant site and an ad-atom on the surface. When the surface is highly stressed as at a crack tip, the degree of surface roughening and the density of ad-atoms is greatly increased. Because of surface forces, the ad-atoms either diffuse along the surface to the crack root or enter the adjacent solution via a dissolution process. Renewed surface roughening at highly stressed bond sites replenishes the surface ad-atom concentration and propogates the crack. This mechanism would lead to the following equation for crack propogation at velocity V_c,

$$V_c = \xi J_R \tag{18a}$$

$$J_R = J_{S.D.} \text{ or } J_D \tag{18b}$$

where J_R is the instantaneous roughening flux, $J_{S.D.}$ is the surface diffusion flux, J_D is the dissolution flux and ξ is a constant for a given crystal face.

It is important to realize how strongly connected is J_R to the excess interfacial free energy, γ. As is well known, the excess energy of a free surface is directly related to the number and energy of the unsatisfied bonds at the surface and this, in turn, is related to the cohesive strength of the material[5]. Likewise, the degree of free surface roughening is directly related to the bond strength and increases exponentially with decrease of bond strength. Thus, one finds that low values of γ correspond to high values of surface roughening. At solid-liquid interfaces, γ is quite low and surface roughening will be especially large. When one deals with an alloy liquid of which one component is surface active, adsorption of that component to the surface lowers γ and increases J_R[6]. In addition, electron transfer between the solid and the liquid will influence J_R. If electrons are transferred from the solid to the liquid in the double layer, J_R is expected to be increased whereas for the reverse direction of electron transfer, the situation is reversed. We can thus see, in an atomistic way, how the environment, temperature and stress level influence the propagation rate of a crack. Let us now look at specifics.

(a) Bond Model for Surface Roughening of Pure Metals

For illustrative purposes, we will consider a simple cubic solid metal

in contact with a liquid metal. On a nearest neighbor (N.N.) picture, each molecule of a simple cubic solid in a (100) interface makes 1 solid-liquid (S/L) bond. The excess energy, E_b, of this double bond over the sum of a solid-solid bond plus a liquid-liquid bond is equal to the excess surface free energy per molecule, f_c, if excess surface entropy effects are neglected. On the basis of a 1st, 2nd and 3rd N.N. bond only picture, in which the bond strengths are related by a 6-12 potential, 1 -1st, 4 - 2nd and 4 - 3rd N.N. bonds with excess energies E_{b_1}, E_{b_2}, E_{b_3} respectively need be considered. Because of the atomic spacing in the S.C. system, $E_{b_2} \approx E_{b_1}/8$ and $E_{b_3} \approx E_{b_1}/27$ so that

$$f_c + TS_c \approx 1.64\, E_{b_1} \tag{19}$$

where S_c is the excess surface entropy. Knowing f_c and S_c, E_{b_1} can be determined. For a free surface without stress, E_{b_1} is related to the cohesive energy, S^*, of the crystal and is given by $E_{b_1} = S^*/7.3$ (6 - 1st, 8 - 2nd, 8 - 3rd N.N.). For this surface in contact with another medium, we expect that

$$E_{b_1} = \frac{1}{7.3}\left[(S_1^* + S_2^*) - E_{12}\right] \tag{20}$$

where the second medium has also been assumed to be S.C. for simplicity and where E_{12} is the energy of interaction of the two media.

For the case of a surface strain of magnitude ϵ, the bond energy in the direction of loading is reduced by $\alpha_i \epsilon^2$ where i = c or t for compression or tension respectively. In the lateral directions, the bond energy is reduced by $d_i \nu^2 \epsilon^2$, where ν is Poisson's ratio. At a free surface, the electron spill-over into the vacuum phase reduces the free electron density per atom so that we may consider r_s in Fig. 1 to have changed for the outer layer of atoms

producing a reduced cohesive strength for this electron condition and thus a smaller value of Eb_1 by $\delta_j \cdot \gamma r_s^2$ where j = + or - depending on the sign of r_s. For a metallic solid in contact with a liquid metal, electron transfer will occur at the interface and a similar effect will be found. The tendency of both stress and electron transfer is to reduce Eb_1.

In the actual process of roughening, an atom in the surface jumps to an ad-atom position at an energy cost of $4Eb_1'$ and leaves behind either a vacancy (free surface) or a vacancy-liquid atom defect at an energy cost of $4Eb_1''$. These energies relate to a 1st N.N. bond model and could be readily extended to 1st, 2nd and 3rd N.N. bond models, etc. For this 3-state model, let X_0, X_1 and X_{-1} be the fraction of molecular states of type 0 (undisturbed), 1 (ad-atom) and -1 (vacancy defect) respectively per unit area of interface. Therefore

$$X_0 + X_1 + X_{-1} = 1 \tag{21}$$

Considering that the formation of (1,1) and (-1,-1) neighbors results in a decrease of one S/environment bond each, the excess energy, Δu, over that of the smooth surface is given by

$$\Delta u = 4\left[E_{b_1}' X_1 (1-X_1) + E_{b_1}'' X_{-1} (1-X_{-1})\right] \tag{22}$$

In calculating Δu, only that portion arising from bonds parallel to the surface need be considered since the number of bonds normal to the surface is unaltered by the presence of states of type +1 and -1. The average entropy change per site is simply determined by the number of arrangements, ω, of the n-sites for fixed X_1 and X_{-1} which is given by $\Delta S = (k/n) \ln \omega$. Thus, we have

$$\Delta S = \frac{k}{n} \ln \left\{ \frac{n!}{(nX_1)!(nX_{-1})!(n(1-X_1-X_{-1}))!} \right\} \tag{22a}$$

$$\Delta S = -k[X_1 \ln X_1 + X_{-1} \ln X_{-1} + (1-X_1-X_{-1}) \ln (1-X_1 - X_{-1})] \quad (22b)$$

and the total free energy change, $\Delta F(X_1, X_{-1})$ due to roughening is given by

$$\Delta F(X_1, X_{-1}) = \Delta u - T\Delta S \quad (23)$$

The optimum degree of diffuseness is given by minimizing ΔF with respect to variations of (X_1, X_{-1}). These optimum values X_1^* and X_{-1}^* are given by

$$\frac{X_1^*}{1-X_1^*-X_{-1}^*} = e^{-\frac{4E'_{b_1}}{kT}(1-2X_1^*)} = \frac{X_1^*}{X_0^*} \quad (24a)$$

$$\frac{X_{-1}^*}{1-X_{-1}^*-X_1^*} = e^{-\frac{4E''_{b_1}}{kT}(1-2X_{-1}^*)} = \frac{X_{-1}^*}{X_0^*} \quad (24b)$$

and

$$\frac{\Delta F(X_1^*, X_{-1}^*)}{kT} = \frac{4}{kT}\left[E'_{b_1} X_1^*(1-X_1^*) + E''_{b_1} X_{-1}^*(1-X_{-1}^*)\right] + X_1^* \ln X_1^* + X_{-1}^* \ln X_{-1}^* + X_0^* \ln X_0^* \quad (24c)$$

For the simple case where $E'_{b_1} = E''_{b_1}$, $X_1^* = X_{-1}^*$, and this is plotted in Fig. 7, versus $E_{b_1}^*/kT$. Here, we can see that if $E_{b_1}^*/kT \lesssim 0.25$, a completely roughened condition prevails. Note that the roughening decreases rapidly for values of $E_{b_1}^*/kT \gtrsim 0.65$ and that an essentially singular surface exists for $E_{b_1}^*/kT > 1.25$. In order to evaluate $E_{b_1}^*$ in general and relate it to some physically measurable quantity, we could assume that the measured surface tension, γ, is given from eqs. 19 and 24 by

$$\gamma = f_c + \Delta F(X_1^*, X_{-1}^*) = 1.64\, E_{b_1} - T S_c + \Delta F(X_1^*, X_{-1}^*) \quad (25)$$

In Fig. 7, both $\Delta F(X^*)$ and $\gamma + TS_c$ are plotted. We can see that small values of γ correspond to small values of $E^*_{b_1}/kT$ and to large values of X^*. Thus, in the liquid metal embrittlement situation, we can see that, because of the very low values of γ, X^* will be large and crack propagation by this mechanism should be very rapid.

(b) Surface Diffusion Aspect

In general, solutions to surface diffusion problems, in which the surface self-diffusion coefficient appears, relate the drift velocity of diffusing atoms to the electrochemical potential gradient through the Einstein relationship

$$v = - (D/kT)(\partial\eta/\partial x) \tag{26}$$

where η is the electrochemical potential of the diffusing species. The diffusion flux is given by the product of the drift velocity and n_D, the concentration of diffusing atoms on the surface. The electrochemical potential gradient is determined by capillarity and other external constraints, so that the final solutions of the diffusion equation depend on surface structure through Dn_D. Comparing diffusion via surface vacancies (where 4 bonds are broken) versus via surface ad-atoms (where only 1 bond is broken), we find that the bond model gives

$$D_s(vac) \approx a^2 \nu \, e^{[-(4E_{b_1} + E_{st})/kT]} \tag{27a}$$

where E_{st} represents the strain energy associated with the displacement of atoms and

$$D_s(ad) \approx a^2 \nu \, e^{-E_{b_1}/kT} \tag{27b}$$

In practice, J(ad) $\gg$ J(vac) so that we need consider only ad-atom diffusion on the surface which will be extremely rapid for small values of E_{b_1}.

We must also evaluate the rate of formation of surface ad-atoms when the population is below its equilibrium level in order to see if this step of the process is rate limiting. The relaxation time, τ, for equilibration by the formation of ad-atoms from atoms in the surface will be

$$\tau = (4\nu)^{-1} e^{5E_{b_1}/kT} \tag{28}$$

which has such small values for those cases wherein X^* is significant ($\tau \sim 10^{-12}$ sec), that we can assume the ad-atom equilibrium concentration at the tip of the crack is maintained during the propagation process.

When one wishes to extend the foregoing to binary alloy systems, it is necessary to consider the detailed thermodynamics of the binary solid and liquid solutions and to determine the interfacial segregation to a smooth interface plus the free energy change associated with this segregation. The next step would then be to determine the changes arising from surface roughening in such an alloy system. The smooth surface study has been carried out under the auspices of this grant and is reported on in Ref. 6. There, the interfacial segregation and the free energy of segregation for solid/liquid interfaces between binary solutions are computed for the (111) boundary of face-centered cubic crystals. A lattice-liquid interfacial model and pair-bonded regular solution model were employed in the treatment with an accommodation for liquid interfacial entropy (which approximately doubles the interfacial free energy).

For unsegregated interfaces, non-ideal solution behavior may significantly change the interfacial free energy. If the heats of mixing are positive or

negative, respectively, the free energy is raised or lowered, respectively, approximately in proportion to the excess of the magnitude of the liquid heat of solution over the magnitude for the solid value. These effects generally increase in proportion to the composition difference of solutions.

Segregation always reduces the interfacial free energy relative to unsegregated interfaces. The free energy is generally raised when the numerical value of the solid heat of solution exceeds or is about equal to that of the liquid. These effects are also increased by compositional difference between the solutions. The zone of compositional transition at the interface generally extends over a few atomic layers and is found to be moderately narrower when the solutions are ideal. Master plots were developed and presented for predicting the segregation and interfacial free energies in general binary systems. The final step of evaluating the change of interfacial roughness for such systems has not been completed so the effect on crack propagation cannot be exactly evaluated. However, as a general rule one can say that, as γ (smooth interface) decreases, the degree of interfacial roughness will increase so that γ (rough interface) will decrease even more strongly and cracking susceptibility will strongly increase.

3. Circulating Currents at the Crack Tip

The inhomogeneous stress distribution at the tip of the crack leads to electron and ion core relaxation which leads to the development of an electrostatic potential, ϕ_s, along the surface of the crack tip. This volume electrostatic potential does not, by itself, cause any electron motion in the solid since ϕ_s is just that needed to produce equilibrium in the solid. However, if we look at the effect of ϕ_s on the charge flow within the inner crack material, the story is quite different. Here, ϕ_s causes the movement of charge

to a degree depending on the conductivity of this inner crack medium. This movement of charge tends to diminish ϕ_s by $\Delta\phi_s$ and $\Delta\phi_s$ drives current through the bulk metal side of the crack. The process continues until a magnitude of $\Delta\phi_s$ is reached wherein a steady circulating current, J, flows around the loop. Since J must be conserved in this process, we have the following equations operating:

$$J_i = J_o \qquad \text{at the surface, S,} \tag{29a}$$

which is equivalently

$$\sigma_i E_i = \sigma_o E_o \qquad \text{at S} \tag{29b}$$

where i and o represent inner and outer crack spaces, σ = electrical conductivity and E is the electric field at S. Finally, for similar distance scale factors, we have

$$\sigma_i(\phi_s - \Delta\phi_s) \approx \sigma_o \Delta\phi_s \tag{29c}$$

For a vacuum at i, $\sigma_o \gg \sigma_i$ and $\Delta\phi_s \approx 0$; for an aqueous film containing an electrolyte at i, $\sigma_o \sim 10^2 - 10^3\ \sigma_i$ so that $\Delta\phi_s \sim 10^{-2} - 10^{-3}\ \phi_s$; for a liquid metal at i, $\sigma_o \sim 2\sigma_i$ so that $\Delta\phi_s \sim \frac{1}{3}\phi_s$. For the aqueous film, we can readily see the importance of polyvalent electrolyte additions on the change of σ_i.

Let us now evaluate the magnitude of the circulating current for these three cases. It is given by

$$J \sim \sigma_i \frac{(\phi_s - \Delta\phi_s)}{\rho^*} \tag{30}$$

where ρ^* is the radius of curvature of the crack tip $\sim 10^{-3} - 10^{-4}$ cm. For

a gaseous inner environment, $\sigma_i \lesssim 10^{-6}$ so that J is negligible; for an aqueous environment, $\sigma_i \sim 10^{-3}$ - 1 so that $J \lesssim 1$ amp/cm^2; for a liquid metal environment, $\sigma_i \sim 10^5$ so that $J \sim 10^6$ - 10^7 amps/cm^2 ($\phi_s \sim 10^{-2}$ volts). This latter current density will have a strong effect on both atomic and vacancy migration in the solid. These values of J are in excess of those needed to produce vacancy coalescence failure in microelectric circuits[7,8] and, therefore, should be of major importance in liquid metal embrittlement.

Besides the atomic migration and void formation effects driven by the electrostatic potential change at the crack surface, one might expect that equilibrium reactions at the surface between solid and liquid will be altered because of both local temperature and potential changes.

References

1. A. J. Dessler, F. C. Michel, H. E. Rorschack and G. T. Trammell, Phys. Rev. 168, No. 3, 737 (1968).
2. D. Pines, "Elementary Excitations in Solids," Ch. 3 (W. A. Benjamin, Inc., New York, 1963).
3. N. D. Lang and W. Kohn, Phys. Rev. 83, 1215 (1971).
4. W. A. Tiller and R. Schrieffer, Scripta Met. 4, 57 (1970).
5. W. A. Tiller, "Treatise on Materials Science and Technology," Vol. 1, p44, editor, H. Herman (Academic Press, New York, 1972).
6. D. Nason and W. A. Tiller, Surface Science 40, 109 (1973).

Figure Captions

1. Typical variation of E_0 and E as a function of r_s, showing cohesive energy S^* and equilibriu atomic radius r_0. I is the ionization energy of the free atom ($E_0 \to I$ as $r_s \to \infty$).
2. Energy diagram for different electron energy levels relative to the zero point energy of the electron at infinity outside the metal.
3. Schematic representation of (a) charge density distribution at a notch surface and (b) various energies relevant to the study of the work function.
4. Variation of electrochemical potential, η_e, as a function of r_s both neglecting and including the Coulomb term.
5. Two samples in vacuum of fixed N and slightly different r_s to illustrate direction of electron flow via two paths.
6. Atomic configuration near the tip of a crack in a simple cubic crystal.
7. Plot of (a) the equilibrium number of +1 states X_1^* for the 3-level and 5-level model of a rough interface for a simple cubic lattice, (b) the decrease in free energy $\Delta F(X^*)$ due to roughening for these models and (c) the interfacial energy γ for the 3-level model all as a function of E_{b_1}/kT where E_{b_1} is the 1st nearest neighbor bond strength.

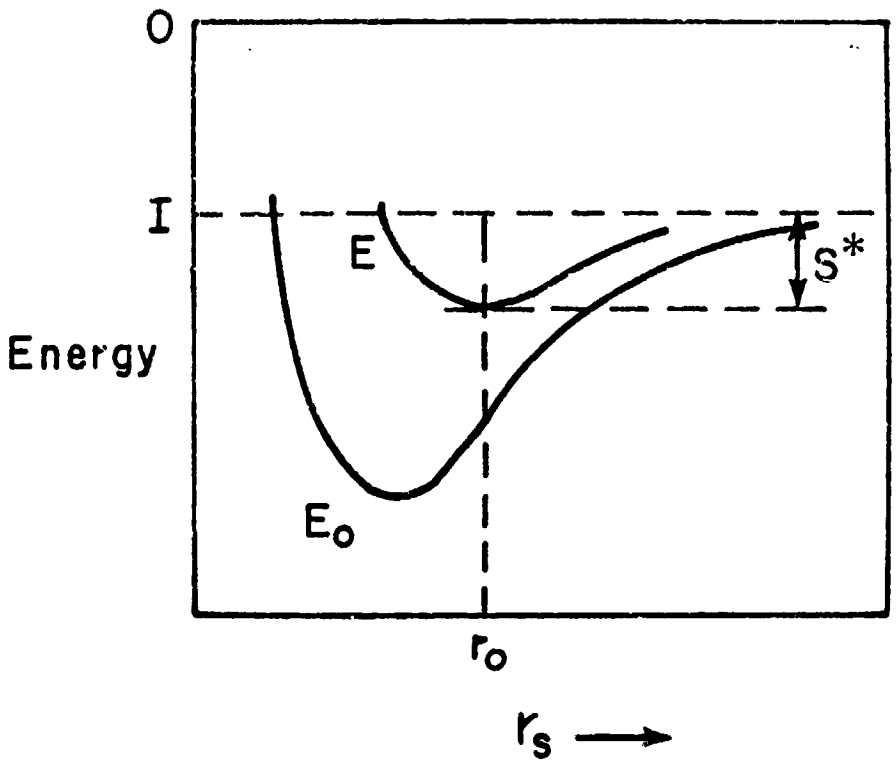

FIGURE 1

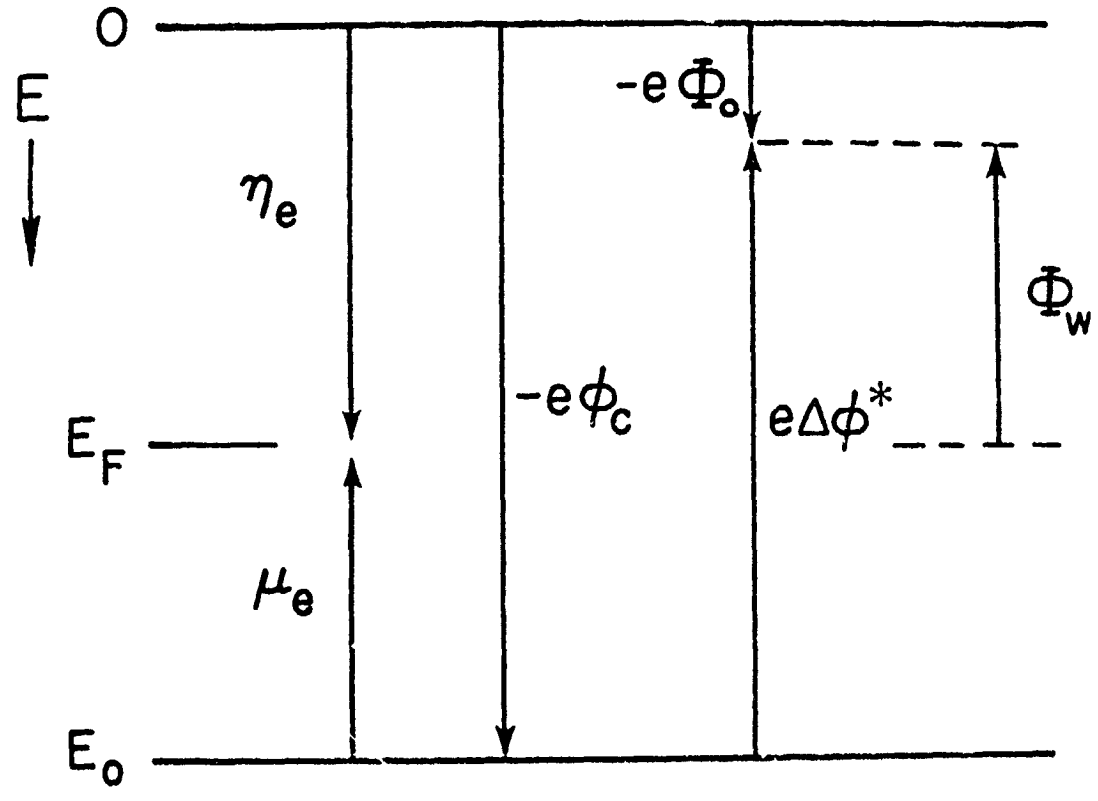

FIGURE 2

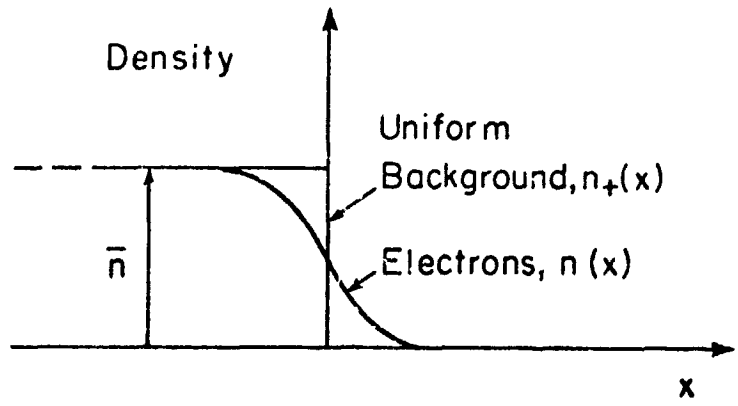
Density
Uniform
Background, $n_+(x)$
$\bar{n}$
Electrons, n (x)
x

(a)

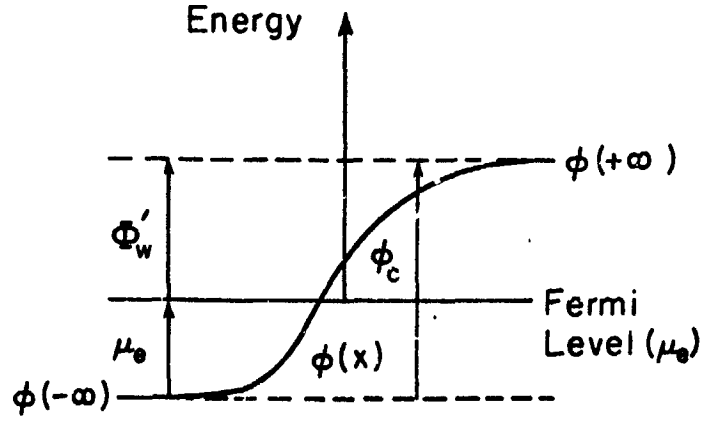
Energy
$\phi(+\infty)$
Φ_w'
ϕ_c
Fermi
Level (μ_e)
μ_e
$\phi(x)$
$\phi(-\infty)$

(b)

FIGURE 3

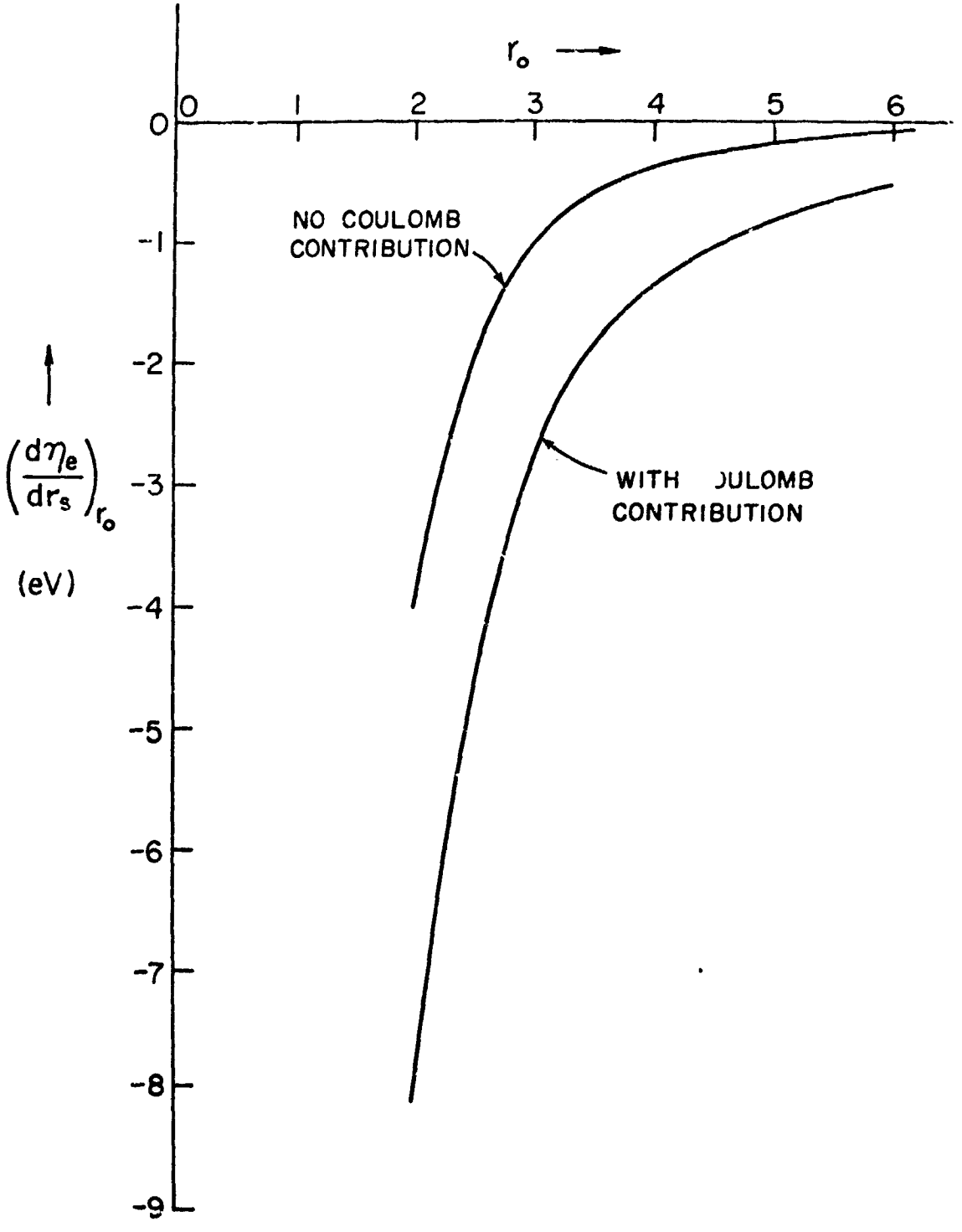
r_o
0
1
2
3
4
5
6
0
-1
-2
-3
-4
-5
-6
-7
-8
-9
NO COULOMB CONTRIBUTION
WITH COULOMB CONTRIBUTION
$\left(\frac{d\eta_e}{dr_s}\right)_{r_o}$
(eV)

FIGURE 4

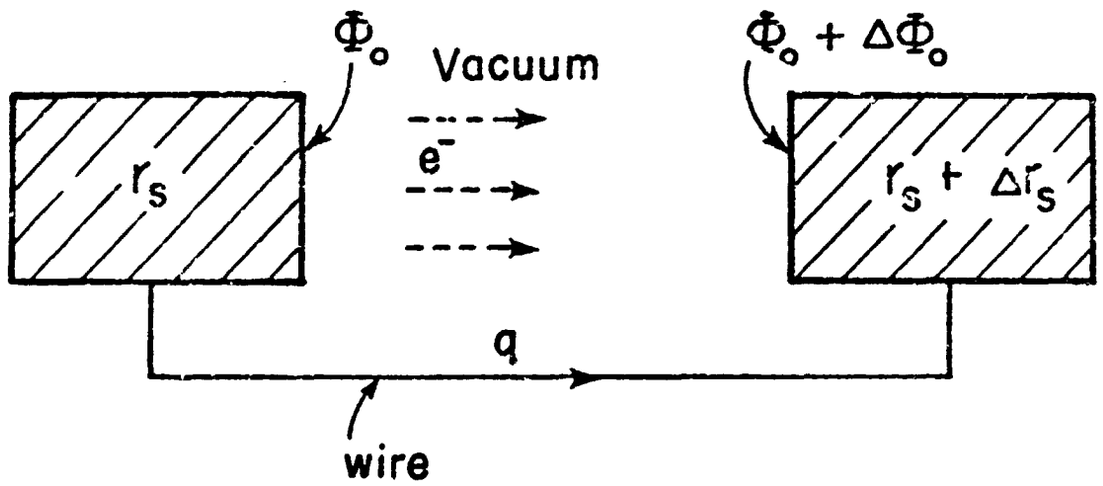

FIGURE 5

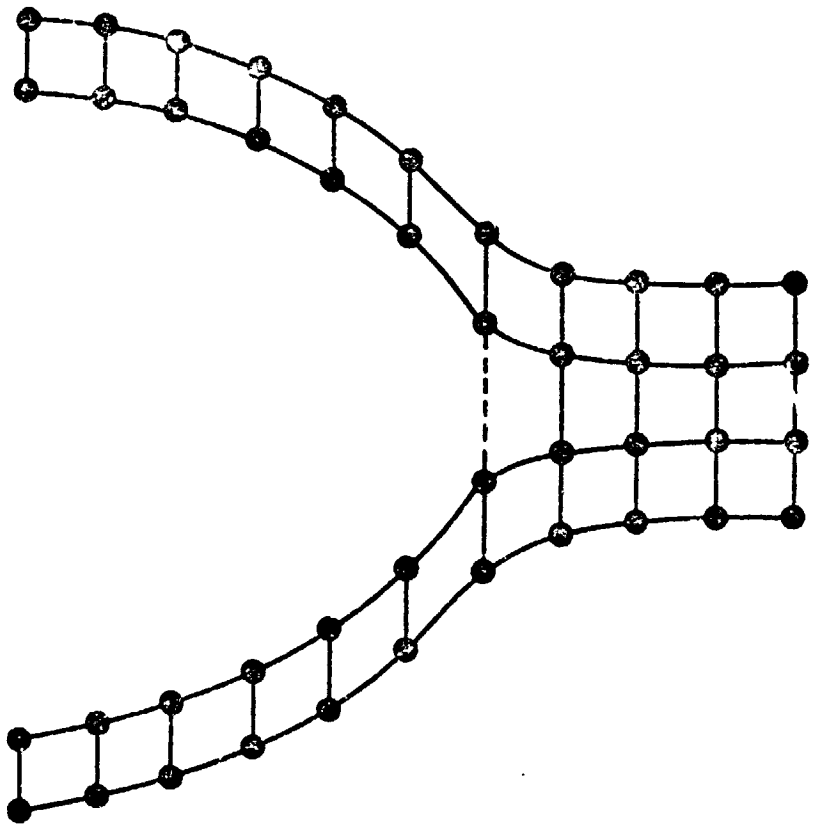

FIGURE 6

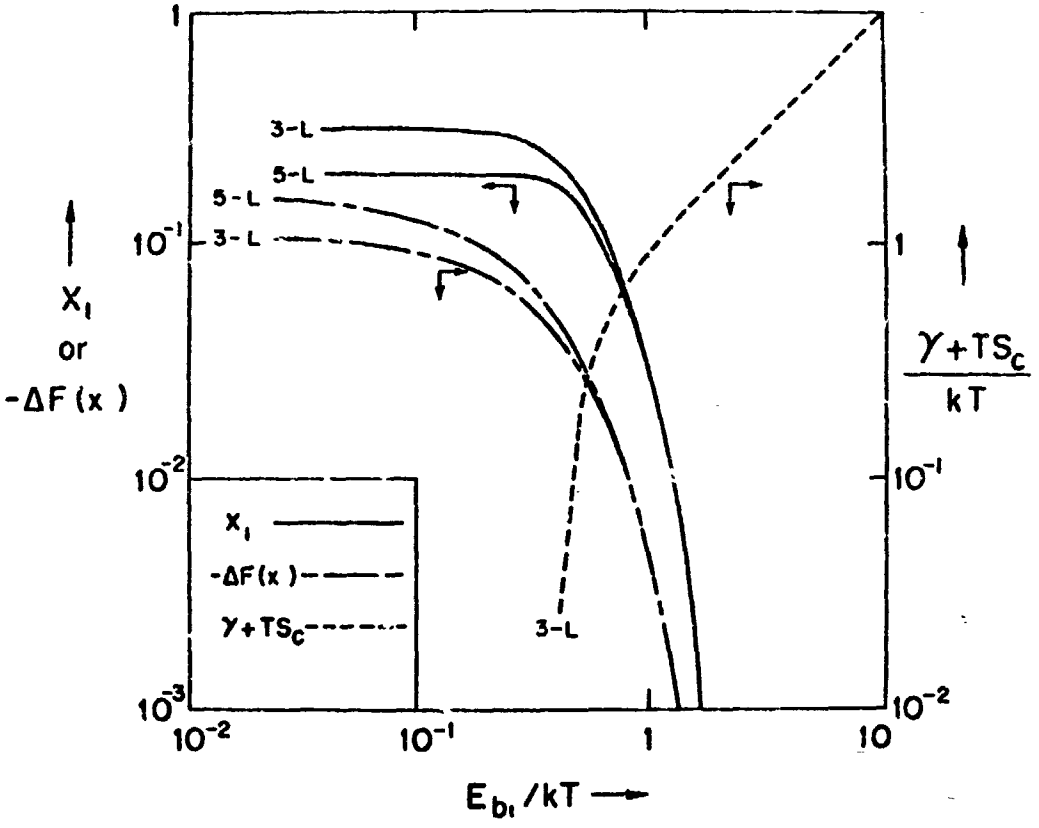
1
3-L
5-L
5-L
3-L
10^{-1}
10^{-2}
10^{-3}
X_1
or
$-\Delta F(x)$
X_1
$-\Delta F(x)$
$\gamma+TS_c$
3-L
1
10^{-1}
10^{-2}
$\frac{\gamma+TS_c}{kT}$
10^{-2}
10^{-1}
1
10
$E_{b_1}/kT \longrightarrow$

FIGURE 7